World Journal of Condensed Matter Physics, 2016, 6, 244-260
Published Online August 2016 in SciRes. http://www.scirp.org/journal/wjcmp
http://dx.doi.org/10.4236/wjcmp.2016.63023

A Different Approach to High-T_c Superconductivity: Indication of Filamentary-Chaotic Conductance and Possible Routes to Room Temperature Superconductivity

Hans Hermann Otto

Materialwissenschaftliche Kristallographie, Clausthal University of Technology, Clausthal-Zellerfeld, Lower Saxony, Germany
Email: hhermann.otto@web.de

Received 26 July 2016; accepted 19 August 2016; published 22 August 2016

Abstract

The empirical relation of $T_{co}(\mathrm{K}) = 2740/\langle q_c \rangle^4$ between the transition temperature of optimum doped superconductors T_{co} and the mean cationic charge $\langle q \rangle_c$, a physical paradox, can be recast to strongly support fractal theories of high-T_c superconductors, thereby applying the finding that the optimum hole concentration of $\sigma_o = 0.229$ can be linked with the universal fractal constant $\delta_1 = 8.72109\ldots$ of the renormalized quadratic *Hénon* map. The transition temperature obviously increases steeply with a domain structure of ever narrower size, characterized by *Fibonacci* numbers. However, also conventional *BCS* superconductors can be scaled with δ_1, exemplified through the energy gap relation $k_B T_c \approx 5\Delta_0/\delta_1$, suggesting a revision of the entire theory of superconductivity. A low mean cationic charge allows the development of a frustrated nano-sized fractal structure of possibly ferroelastic nature delivering nano-channels for very fast charge transport, in common for both high-T_c superconductor and organic-inorganic halide perovskite solar materials. With this backing superconductivity above room temperature can be conceived for synthetic sandwich structures of $\langle q \rangle_c$ less than 2+. For instance, composites of tenorite and cuprite respectively tenorite and CuI (CuBr, CuCl) onto AuCu alloys are proposed. This specification is suggested by previously described filamentary superconductivity of "bulk" CuO_{1-x} samples. In addition, cesium substitution in the Tl-1223 compound is an option.

Keywords

Superconductivity, Fractals, Chaos, Feigenbaum Numbers, Fibonacci Numbers, Golden Mean,

How to cite this paper: Otto, H.H. (2016) A Different Approach to High-T_c Superconductivity: Indication of Filamentary-Chaotic Conductance and Possible Routes to Room Temperature Superconductivity. *World Journal of Condensed Matter Physics*, **6**, 244-260. http://dx.doi.org/10.4236/wjcmp.2016.63023

Ferroelastic Domains, Mean Cationic Charge, Perovskites, Cuprates, Tenorite, Cuprite, Cesium Substitution, Solar Power Conversion Efficiency

1. Introduction

The recent discovery of conventional superconductivity at the highest until today known transition temperature of 190 K on hydrogen sulfide at a high pressure >150 GPa by Drozdov, Eremets and Troyan (2014) [1] gives rise to discuss again a possible route to superconductivity above room temperature. However, high pressure is not recommended for everyday use. Very recently, the crystal structure of this high pressure modification of H_2S was solved, indicating an anti-perovskite structure in the sense that SH^- represents the A site and SH_3^+ the B site of this structure type [2]. Below I will suggest a hypothetical anti-perovskite compound that would, if chemically accessible, a highly interesting option for a room temperature superconductor. Some years ago we published an experiment, which indicated filamentary, but not stable superconductivity at 220 K of an oriented multi-phase sample of the Y-Ba-Cu-O system, deposited on a (110)-$SrTiO_3$ substrate (Schönberger *et al.*, 1991) [3]. The uncommon (110) orientation of the substrate surface was chosen to provoke symmetry reduction and ferroelastic domain formation of the deposited thin film phases by strain. We identified the minor compounds $BaCuO_2$ and CuO, respectively, besides the superconducting main phase $YBa_2Cu_3O_{7-\delta}$. A comparable result with a large resistivity drop at 220 K has been published little earlier by Azzoni *et al.* (1990) [4] on reduced cupric oxide samples, which showed some red Cu_2O besides CuO. Later Osipov *et al.* (2001) [5] deposited Cu films onto cleaned CuO single crystal surfaces and observed at the CuO-Cu interface a giant electric conductivity increase by a factor up to 1.5×10^5 even at 300 K. Today it is assumed that the observed rapid drop of the electric resistivity at 220 K and 300 K is caused by superconductivity of oxygen deficient $CuO_{1-\delta}$ filaments [3]-[5]. Consequently, this finding has been patented, by others, as ultra-conductor of bundled filaments of copper oxide coated copper wires and foils, respectively [6].

Interestingly, artificial interfaces between insolating perovskites that indicate superconducting response are described in 2007 by Reyen *et al.* [7]. Further, I quote an investigation published recently by Rhim *et al.* (2015) [8] regarding possible superconductivity via excitonic pairing onto an interfacial structure between CuCl and Si(111), remembering that electronic anomalies in cuprous chloride have been described by Chu *et al.* [9] long time ago. Both publications encouraged me even more to put earlier ideas about copper oxide composites on record.

A hypothetical $BaCuO_2$ phase with puckered T-CuO nets, in contrast to planar CuO_2 nets of the $BaCuO_2$ infinite layer phase, was recently proposed by the present author as an alternative high-T_c candidate together with a large cupric oxide cluster compound [10]. However, sandwich structures composed of tenorite and cuprite as well as tenorite and CuI respectively CuBr or CuCl are more interesting. Also cesium substitution in the Tl-1223 compound is a route to reach a high transition temperature. The composition for such composites will be passed by the empirical relation of $T_{co} = 2740 \big/ \langle q \rangle_c^4$ that connects the transition temperature T_{co} of optimum doped superconductors with the mean cationic charge $\langle q \rangle_c$ [11]. Moreover, this paradox relation will be traced back to a physically more accepted basis. Both the theoretical results and the practical suggestions regarding T-CuO nets with twice as many copper atoms as in the CuO_2 nets should envisage physicists to realize a dream of mankind, superconductivity above room temperature.

This work was pre-published in *arXiv* just as the message about an apparently successful synthesis of a room temperature superconductor (with far withheld information about chemical composition!) astonishing the scientific community [12]. Therefore, some results may already be outdated, what I don't hope yet, because nature never puts all eggs in one basket.

2. Results and Discussion

The most abundant mineral in Earth is $MgSiO_3$, a perovskite phase confined to the high pressure region of the Earth mantle, but also discovered in a shocked meteorite and now named bridgmanite [13]. The dominance of perovskites and derived phases continues in our technology determined life due to their wide variety of adapted symmetries and the surprising diversity of physical properties such as ferrolectricity, ferroelasticity, supercon-

ductivity, ionic conductivity, photocatalytic property and efficient photovoltaic respond, respectively. Some of these properties are mutually dependent.

Beginning with the last mentioned challenge, the development of efficient solar cells, you just witnessed the great progress in organic inorganic halide perovskite solar cells. Their very high solar efficiency is caused by the low cationic charge of $\langle q \rangle_c = 1.5^+$, resulting in a low and less confining *Madelung* potential that favors a small-sized ferroelastic and conductive domain structure with enhanced charge separation and improved carrier lifetime [14].

2.1. Resolving a Paradox: $T_{co}(\mathrm{K}) = 2740/\langle q_c \rangle^4$

A less restricted freedom of electronic movement may also be suggested for the family of superconductors related to oxide perovskites. The rise of the transition temperature T_{co} goes inversely proportional with the fourth power of the mean cationic charge $\langle q \rangle_c$. **Figure 1** depicts $\langle q \rangle_c$ versus T_{co}, somewhat simplified compared to previous results [11] and now branched into electron (conventional) conductors and hole (unconventional) conductors. The more complicated relation given in the earlier paper was induced by the idea to cover both conventional and unconventional superconductors and by the assumption that a mean cationic charge of 2+ would be a natural crystal-chemical limit. Remarkably, the data summarized in that reference show also exemplarily pnictide-based superconductors. The data given in reference [11] were now supplemented with samples marked with red squares, especially including CuO_{1-x} as hole conductor (*p*-type conductivity), and with the result for H_2S under high pressure as electron conductor (*n*-type conductivity). The curve for electron transport will be discussed in a forthcoming contribution, especially considering the fractal structure of *BCS* superconductivity. The magenta colored curve for hole superconductors (**Figure 1**) is represented by the relation

$$T_{co}(\mathrm{K}) = 2740/\langle q_c \rangle^4 . \quad (1)$$

Surprisingly, $\langle q \rangle_c \approx 1.5^+$ emerges as high-T_{co} asymptotic limit. With a successive reduction of the mean cationic charge in direction of $\langle q \rangle_c = 1.75$ one would reaches the field of possible room temperature superconductivity. Recently, the author proposed hypothetical compound, a cagy cuprate cluster compound as well as

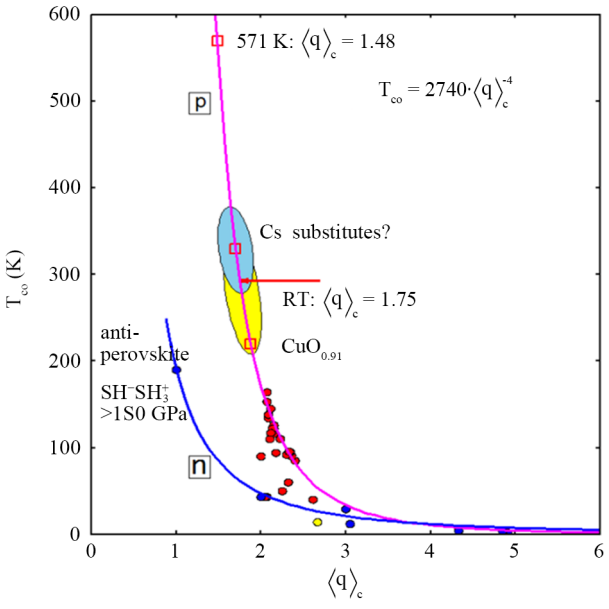

Figure 1. Mean cationic charge $\langle q \rangle_c$ versus transition temperature T_{co} (K) of optimal doped superconductors (see also [11]). Branch of *n*-type superconductors blue, *p*-type ones red. Yellow circle spinel phase superconductor, colored ellipses: composites explained in the text. The *n*-type branch yields $T_{co} = 190/\langle q_c \rangle^2$.

tetragonal $BaCuO_2$ with puckered T-CuO nets [10]. Both compounds could reach a transition temperature around 180 K, if their synthesis with sufficient doping would be successful.

The scale factor of Equation (1) of s_c = 2740 K can intuitively traced back to give

$$s_c = 8\varepsilon^2 m_e \frac{v_F^4}{v_K^2}\frac{1}{k_B} = 2736 \text{ K} \tag{2}$$

where $v_K = \dfrac{e^2}{\varepsilon_o h} = 4.37538\times 10^6$ m/s is a universal constant with the dimension of a speed, e the elementary charge, h the Planck constant, v_F the *Fermi* speed, ε the permittivity of the medium, ε_o the permittivity of free space, and m_e the electron mass, respectively. With ε = 5.04 and an assumed *Fermi* speed of $v_F = 2.5 \times 10^5$ m/s, respectively, the scaling factor agrees well with the fitted parameter of 2740 K. If a higher effective mass of the quasiparticles is chosen, for instance $m_h \approx 1.5 m_e$ (or $m_h = \varphi \cdot m_e$ with φ = 1.61803), then the *Fermi* velocity has to be reduced correspondingly, as was observed experimentally in the region of optimal doping. With $\tilde{v}^2 = v_F^4 / v_K^2$ the result yields

$$k_B T_{co} = \frac{16\varepsilon^2}{\langle q \rangle^4}\frac{1}{2} m\tilde{v}^2 . \tag{3}$$

This represents rather the total energy of a system of oscillating charged quasiparticles, dispersed in a medium of permittivity ε, than solely coulomb energy. The dimensionless variable $\langle q \rangle_c$, with the fourth power instead of the expected second one (in three dimensions of space), obviously subsumes, beside the cationic charges and the hole concentration, also camouflaged anionic contributions and the effect of steadily increasing permittivity, because the compounds of highest T_{co} are composed of highly polarizable heavy atom ions. How the matter might be, the relation between T_{co} and $\langle q \rangle_c$ can serve to predict possible critical temperatures solely from charges of a compound. Besides a low cationic charge a high permittivity (indicating certain proximity to phase transitions) may favorable to support high T_{co}.

Some ideas should be passed on that are related to optimum values of the hole concentration found, and to obvious accumulations in certain T_{co} values. Beginning with the value of optimum h^+ of σ_o = 0.229 (or multiples) [15] that is near 3/13 and is attributed to a large group of high-T_c superconductors based on Tl or Hg, respectively. Surprisingly, the multiplier, which would give two holes needed to create a pair, emerges as the number

$$\delta_1 = 8.721$$

known as a universal scaling constant for two-dimensional maps in the theory of fractal systems or chaotic ones, with the precise value of δ_1 = 8.7210972··· [16] [17]. Recently, Savin *et al*. [18] studied the self-oscillating system of the Van der Pol oscillator [19] subjected to an external force to compensate dissipation. Scaling constants δ_1 (and δ_2 = 2) have been determined as eigenvalues of the matrix containing the existence intervals of two subsequent cycles of the periodic-doubling cascade in the parameterized version of a quadratic *Hénon* map with renormalized (x, y)-parameters.

The optimum concentration of holes is given per cuprate layer per unit-cell. Maintaining two dimensions along cuprate layers, then two electrons reside in a slab of the extension $\delta_1 a^2 = \pi l^2 a^2$. The "domain" extension multiplier is then given by the quotient of *Fibonacci* numbers

$$l = \sqrt{(\delta_1/\pi)} \approx 5/3 . \tag{4}$$

Pnictide superconductors yield an optimum hole concentration of about $\sigma_o/4$ [15] and can be traced back to δ_1 too. Further, although it is already difficult to identify optimum doping, picking out accumulations in the T_{co} ranking is the more difficult. Nevertheless, one can try it as Mitin [20] has done before, identifying such T_{co} groups with domain widths. This author related the transition temperature T_{co} to assumed zig-zag bosonic stripe domains of width $w = \eta \cdot a$ that are connected with oxygen interstitials. He obtained

$$T_{co} = \frac{h^2}{32\pi^2 m_e r_o^2 k_B \left(2\eta^2 + \eta\right)} \tag{5}$$

where h represents the *Planck* constant, k_B the *Boltzmann* constant, m_e the rest mass of the electron, a an ele-

mentary length related to neighboring cations, r_o = 2.72 Å a string distance along O-O bonds, and $f(\eta)=\sqrt{(2\eta^2+\eta)}$ a function of the domain extension (rank) η with respect to a, respectively.

Going a step further, one can associate such T_{co} clumps with *Fibonacci* numbers f_i determining the extension of domains. Possible mixed domain states can be described by the mean of consecutive f_i's. **Table 1** compares *Mitin*'s results with my *Fibonacci* number explanation. The results may give a hint to a possible filamentary-chaotic origin of high-T_c superconductivity. Using *Fibonacci* numbers f_i one can roughly formulate (see **Table 1**):

$$T_{co} \approx 12000/f_i(\mathrm{K}). \tag{6}$$

Upon substitution of Equation (1) into Equation (6) one gets

$$\langle q\rangle_c^4 = 0.228\cdot f_i \approx 2f_i/\delta_1 . \tag{7}$$

Surprisingly, the emerging factor corresponds numerically to the charge of σ_o = 0.228 [15]. It is remarkable that also the quotient of the *Fermi* speed chosen (which is near to reality) and the *Klitzing* speed yields

$$v_F/v_K \approx 0.0571 \approx 1/(4\sigma_o) \approx 1/(2\delta_1). \tag{8}$$

With this result one can finally express the energy in different and scale-free forms:

$$k_B T_{co} \approx \frac{8\varepsilon^2}{f_i\sigma_o} m_e \tilde{v}^2 \cdot k_B T_{co} \approx \frac{\varepsilon^2}{f_i\delta_1} m_e v_F^2 \cdot k_B T_{co} \approx \frac{\varepsilon^2}{4 f_i \delta_1^3} m_e v_K^2 . \tag{9}$$

Table 1. Dependence of the superconducting transition temperatures T_{co} on the domain width $w = \eta\cdot a$, $f(\eta)^2 = 2\eta^2 + \eta$, where η represents the rank introduced by Mitin [20], f_i = *Fibonacci* numbers.

η	d_i		Mean of consecutive f_i's	T_{co}	$T_{co}\cdot d_i$	$\langle q\rangle_c$
	$2\eta^2+\eta$	f_i				
		8		(1500)	12,000	-
2	10		10.5	(1200)	12,000	-
		13		(923)	12,000	-
3	**21**	**21**		**571**	11,991	1.48
4	**36**	**34**		**353** **334**	12,000 12,024	1.67 1.70
5	**55**	**55**		**219**	12,045	1.87
6	**78**		72	**167** **155***	12,024 12,090	2.01 2.05
		89		**135**	12,015	2.12
7	**105**			**115**	12,075	2.21
			116.5	103	12,000	2.26
8	**136**	**144**		**89** **84**	12,104 12,096	2.35 2.39
9	**171**			**70**	11,970	2.50
			188.5	64	12,064	2.55
10	**210**	**233**		**57** **52**	12,000 12,116	2.63 2.70
11	**253**			**47**	12,000	2.76
12	**300**		305	**40**	12,000	2.88

*High pressure applied.

When using the conductance quantum $G_o = 2e^2/h = 7.748091 \times 10^{-5}$ (S) one can write down the energy as

$$k_B T_{co} \approx \frac{\varepsilon^2}{16\varepsilon_o^2 f_i \delta_1^3} m_e G_o^2 \tag{10}$$

The multiple energy representation is given by the special nesting property of fractals. Resolving the paradox finally leads to the result that high-T_c superconductors obey fractal conductance behavior, which is intrinsically accompanied with self-similarity and scale-free characteristics. This finding of possible fractality and self-similarity of high-T_c superconductors supports the seminal investigations of Fratini *et al*. [21] on the fractal organization of oxygen interstitials and the recent contribution of Poccia *et al*. [22]. Later Phillabaum *et al*. [23] reported on the fractal structure of nanoscale electron lines on the surface of superconductors that spread out in the bulk. In this context I quote also the zig-zag filamentary theory of high-T_c superconductors of *Phillips* [24] [25].

If the domain width lessens, then the ratio of its surface to volume will be enlarged. This ratio is thought to be scaled by the golden mean, $\varphi = \left(\sqrt{5}+1\right)\big/2 = 1.618034$. In addition, a large surface may support a certain quality to act as particle detector.

It remains to be emphasized that the energy $k_B T_c$ of conventional *BCS* superconductors can also be formulated using an inverse δ_1 scaling applied to the energy gap Δ_0 at $T = 0$ K [26], giving the relation (11)

$$k_B T_c\left(BCS\right) \approx 5\Delta_0/\delta_1$$

$2\Delta_0$ is the energy required to break a *Cooper* pair. The *BCS* superconducting gap has s-wave symmetry and shows minimal momentum dependence.

Recently, Mushkolaj [27] compared two mutually inverse T_c functions related to an elastic atom collision model in contrast to an elastic spring model, respectively, given by

$$T_c\left(\text{collision}\right) \propto z^{-1} \text{ versus } T_c\left(\text{spring}\right) \propto z\,, \tag{12}$$

where $z = \left(\sqrt{M_1 M_2}\right)\Delta x^2$, and M_i = atom or electron masses, Δx = distances. However, the picture of colliding point particles should be replaced by nested highly coherent vibrations of most irrational frequency, a superposition of inwardly and outwardly extending spherical quantum waves in the sense of Wollf's conjecture for the electron [28]. Indeed, solutions of the rational function $f\left(z\right) = z - z^{-1}$, which may describe competition between both underlying physical processes (Equation (12)), would point to chaotic behavior of the excited carriers. Analogously, the most irrational number of the golden mean, $\varphi = \left(\sqrt{5}+1\right)\big/2 = 1.618033988\cdots$, is related to its inverse by $\varphi - \varphi^{-1} = 1$, or generalized, by $\varphi^i \pm \varphi^{-i} = f_i + f_{i+2}$ with *Fibonacci* sequence numbers $f_i = 0, 1, 1, 2, 3, 5, 8\cdots$ (±: +if i = even else −). This divine number is connected with chaos respectively fractal structures and self-similarity. The transfinite golden mean is most suitable to describe comprehensively our self-similar universe because of the proper connection of that number with its inverse. Philosophically formulated, since the big bang the diverging matter (and energy) is retracted again at the same time by an inverse process.

2.2. Playing with Fractal Numbers

Both universal constants δ_1 and the golden mean φ, respectively, can be connected by the approximate relation

$$\varphi^5 \approx 4\delta_1/\pi\,. \tag{13}$$

Using this result, one can approximately express δ_1 as a quite catchy product of three fundamental constants together with a denominator as a product of *Fibonacci* sequence numbers:

$$\delta_1/3 \approx \pi \cdot \varphi \cdot \bar{\alpha}_o \big/ \left(1 \cdot 2 \cdot 3 \cdot 5 \cdot 8\right), \tag{14}$$

where

$$\bar{\alpha}_o = \varphi^4 \cdot 20 = 137 + \varphi^{-3}\left(1 - \varphi^{-3}\right)\big/2 = 137.082039 \tag{15}$$

represents the inverse of *Sommerfeld*'s dimensionless fine structure constant as given in El Naschie's E-infinity theory [29]. However, the experimental value is best reproduced by $\bar{\alpha}_o = 137 + \varphi^{-3}\left(1 - \varphi^{-3}\right)\big/5 = 137.036$, whereas one calculates $\bar{\alpha}_o = 137.254$ something too big when using δ_1. The number 137 itself is the 33rd prime number.

The golden mean respectively $\bar{\alpha}_o$ can be applied to mass relations of elementary particles. I will use such relations in chapter 2.3. As an example, the mass of the neutron can be found as [29]

$$m(n) = 20\varphi^8 = (\bar{\alpha}_o)^2 / 20 = 939.574275 \text{ MeV/c}^2 \approx 939.5645133(58) \text{MeV/c}^2 . \quad (16)$$

Further, the fourth power of the golden mean φ^4 applied to the υ_τ lepton mass $m(\upsilon_\tau)$ = 15.4214 MeV/c^2 gives the mass of the μ lepton:

$$m(\mu) = \varphi^4 m(\upsilon_\tau) = m(\upsilon_\tau) / (20\alpha_o) = 105.7 \text{ MeV/c}^2 . \quad (17)$$

The mass ratio of the υ_τ particle to the electron yields

$$m(\upsilon_\tau) / m(\text{e}) = 30.178 \approx \varphi^5 \exp(1) \approx 4\delta_1 \exp(1)/\pi \approx 2\delta_1^2 / 5 . \quad (18)$$

In this way, the universal *Feigenbaum* constant δ_1 of the quadratic *Hénon* map, explained before, is apparently involved in mass relations between elementary lepton particles.

2.3. Superconducting Pairing Glue

A majority of high-T_c superconducting compounds shows a pronounced deviation from the tetragonal symmetry. This supports the formation of ferroelastic domains with walls as charge carrier sink. If the itinerant holes formed by doping travel to the walls, it results at the first moment a stack of positively charged walls separating insulating regions. The repulsive forces have to keep in balance and may strengthen orthorhombicity. However, when the concentration of holes exceeds a certain limit, then repulsive forces will be reduces by the formation of bosons, confining preformed pairs of holes in one-dimensional bosonic stripes [30]. One might expect that lowering of the effective cationic charge in the region between the stripes would favor undulation of the stripes, finally leading to the superconducting state due to their interaction.

However, in which way interstitial oxygen ions could be involved in the pairing scenario? A possible modified exciton pairing mechanism may be as follows. In the vicinity of the large and highly polarizable Ba^{2+} ions the oxygen interstitials may show a "chameleon" feature, being once −1 charged and then again −2, respectively. It means that this oxygen atom is able to easily expel or souk a charge carrier. Apical oxygen atoms on the interlayer between cuprate layers and spacer layer can be involved in this process. Just when the apical oxygen atom is displaced towards the Cu center, enough space is provided to create the larger O^{1-} ion. An exciton may bind a just expelled (hot) hole to form a metastable three-particle-entity that would rapidly decay, leaving a boson and the mediating electron, but could also survive as quantum wave composite and would then be observable. It needs only few electrons to form a cascade of bosons, and the probability it happens is higher than for an exciton-exciton process. The pairing process can take place locally near interstitial oxygen atoms or within the strain field of ferroelastic domain wall sinks, involving strain effect as important too.

When the mass of holes is assumed to be $1.5m_e$ in accordance with experimental results [15], then the mass of a conceived composite particle or quantum wave composite of two holes and an electron would be $4m_e$. Intuitively, this special mass multiple of an electron can be depicted alternatively by a third power golden mean representation, because $4m_e = (\varphi^3 - \varphi^{-3}) \cdot m_e$. Such thought experiment suggests the possibility of fractal-based pairing.

The given ideas about fractality of high-T_c superconductors and a modified pairing mechanics, respectively, should be considered in a modified and more founded theory. However, despite the undoubtedly achieved great success of research on high-T_c superconductivity, the impression is still given that the forest is not seen for the trees.

So other concepts may be chosen to go ahead. For instance, a heretical concept may assume an influence of high-T_c superconductivity from the cold. As noticed before, high-T_c superconductors may act as extremely effective "particle" detectors. It remains open to be conjectured that a (less divine) ghostly subatomic "particle" could help to overcome teething problems of pairing, so to speak, an interaction from the dark universe to upset physicists.

If such influence would ever be conceivable, then it would clearly lead to a chaotic response, for instance filamentary-chaotic conductance with self-similar characteristic. Furthermore, a scaling of the pairing vigor down the flight of stairs determined by *Fibonacci* levels (domains) is easy to imagine.

Until then we can work with the auxiliary variable $\langle q \rangle_c$ as a tool to find candidate systems for superconduc-

tivity above room temperature, besides taking care of a high permittivity of the compounds. This is accomplished in the next chapter.

2.4. Routes to Superconductivity above Room Temperature

First, the T_{co} versus mean cationic relation will be applied to make progress with known Tl-based superconductors with CuO_2-based nets. Following this, tenorite-based composites are prospected in detail with twice as many copper atoms per layer.

2.4.1. A Cs-Substituted Tl-1223 Compound

In short, a resume of the crystal-chemistry of Tl-based superconductors will be given. Crystal-chemical data from own structure determinations on Tl-based cuprates were summarized in **Table 2** [31]-[33]. The reduced electron density found at the Tl position of TlO-double layer compounds is recast in partial occupation by Cu^{1+}, and the enhanced value at the Ca position was attributed to a partial Tl^{3+} substitution. The Cu^{1+} content in the calculated amount was confirmed by electron energy loss spectroscopy (*EELS*) on single crystals [34]. What happens, if cations such as Hg^{2+} or Tl^{3+} attain the lower oxidation state with lone electron pairs and associated dipole momentum? The properties of Bi^{3+} are dominated by both the space that the lone electron pair needed and the resulting dipole momentum. Therefore, Bi^{3+} will be shared in *Aurivillius* double-layers, triple domains or channels to minimize the dipole momentum. Indeed, only double layer Bi-based superconductors are found. In the case of Hg^{1+} two ions join to form Hg_2^{2+} with zero resulting dipole momentum, but this was not observed in Hg-based superconductors. If one considers partial replacement of Tl^{3+} by Tl^{1+} in high-T_c superconductors, again one is faced with the effect of the dipole momentum of Tl^{1+}, especially if mono-layer compounds such as Tl-1223 are considered. The replacement should be significantly less than halve the Tl content as observed, but may be restricted to the Tl site and not to the Ca site substitution. Because Tl-1223, given as example in **Table 3**, seemed to be over-doped according to our results, a rescaling was carried out, considering the somewhat reduced Tl bond strength [35] and the site occupation. The site occupation was found little too high, which may be to the higher scattering power of Tl^{1+} compared to Tl^{3+}. The changes are recently summarized [36].

Table 2. Calculation of the hole concentration h^+, the mean cationic charge $\langle q \rangle_c$, and the critical length ζ, using own crystal-chemical data of Tl-based cuprates as examples.

Phase symbol	Tl-2201	Tl-2212	Tl-2223	Tl-1223
a (Å)	3.8656 (3)	3.8565 (4)	3.8498 (4)	3.848 (4)
c (Å)	23.2247 (18)	29.326 (3)	35.638 (4)	15.890 (10)
n	1	2	3	3
f	0	0	0	0.092
x	0.11	0.31	0.42	0
y	-	0.10	0.07	0.069
δ	0	0	0	0.18
h^+	0.220	0.52	0.700	0.686
h^+/n	0.220	0.26	0.233	0.229
$\langle q \rangle_c$	2.353	2.211	2.144	2.12
ζ (Å) Ba-O $\parallel c$	1.945	2.014	2.010	2.073
$T_{co} = 2740/\langle q_c \rangle^4$	88.9	114.6	130	136
$T_{co} = 1247.5 \cdot \sqrt{h^+}/(a \cdot \zeta)$	77.8	115.8	135	130
T_c (K) measured	80	110	130	133
Refs.	[32]	[32]	[30]	[33] [36]

Table 3. Calculation exercise of Cs^{1+} substitution in the Tl-1223 model compound. The first elected substitution corresponds to the actual Tl-1223 composition, merely with a small amount of Cs^{1+} instead of Tl^{1+}.

Notation	Cations							Anions	
Formula subscripts	1		2		2		3	9	
Elements	Tl^{3+}	Cs^{1+}	Ba^{2+}	Cs^{1+}	Ca^{2+}	Tl^{3+}	Cu^{2+}	O^{2-}	F^{1-}
Substitution	0.908	0.092	2	−	1.862	0.138	3	8.82	−
Charge	+2.724	0.092	+4	−	+3.724	+0.414	+6	−17.64	−
$h^+ = 0.686$				$\langle q \rangle_c = 2.12$				$T_{co} = 136$ K	
Substitution	0.75	0.25	2	−	1.862	0.138	3	8.33	0.67
Charge	+2.25	+0.25	+4	−	+3.724	+0.414	+6	−16.6	−0.7
$h^+ = 0.692$				$\langle q \rangle_c = 2.080$				$T_{co} = 146$ K	
Substitution	0.5	0.5	2	−	1.862	0.138	3	7.82	1.18
Charge	+1.5	+0.5	+4	−	+3.724	+0.414	+6	−15.64	−1.18
$h^+ = 0.682$				$\langle q \rangle_c = 2.017$				$T_{co} = 166$ K	
Substitution	−	1	0.9	1.1	2	−	3	5.59	3.41
Charge	−	+1	+1.8	+1.1	+4	−	+6	−11.18	−3.41
$h^+ = 0.690$				$\langle q \rangle_c = 1.738$				$T_{co} = 300$ K	

The complex chemical formula for the homologous series of Tl^{3+}-based superconductors may be written as

$$Tl^{3+}_{m-f-x}Tl^{1+}_{f}M^{s+}_{x}\left(Ba,Sr\right)_2\left(Ca_{1-y}Tl^{3+}_{y}\right)_{n-1}Cu_nO_{m+2n+2-\delta},\ n=1,2,3,\cdots$$

m = 1:TlO mono-layers (space group P4/mmm), m = 2:TlO bi-layers (space group I4/mmm). The space group notation is that of the "averaged" structures.

The hole concentration h^+ then yields

$$h^+ = 2-m+2f+x\left(3-s\right)-\left(n-1\right)y-2\delta\ .$$

Subtracting h^+ from the total charge of oxygen, taken as O^{2-}, the total cationic charge results. The mean cationic charge is calculated by division of the number of cations as

$$\left\langle q_c \right\rangle = 2\left(m+2n+2-\delta\right)-h^+/\left(m+2n+1\right).$$

The amount of lethally toxic Tl^{1+} besides Tl^{3+}may easily be replaced by the environmentally benign Rb^{1+} or Cs^{1+} cations of comparable size (**Figure 2**), if you do not even use the ^{137}Cs isotope, without alter the charge balance. However, further replacement of Tl^{3+} and Ba^{2+}, respectively, by these alkali earth cations would reduce the mean cationic charge $\langle q \rangle_c$ and, according to the Equation (1), should enhance T_c. Such replacement may be further supported by substitution of some oxygen by group VII anions like F^{1-} or more polarizable ones such as Br^{1-} or even I^{1-}. Fluorine substitution was already successfully applied in Bi-based superconductors [37], and-din Hg-based compounds under high pressure with the highest T_{co} known [38] [39]. Fluorine substitution causes shrinkage of the lattice parameters and enhances T_c to its optimum due to internal "chemical" pressure. In **Table 3** some Cs^{1+} and F^{1-} substitutions are proposed assuming the possible adaption of a stable perovskite-related crystal structure.

A Cs-1223 compound of the formula $Cs(Cs_{1.1}Ba_{0.9})Ca_2Cu_3O_{5.6}F_{3.4}$ with an optimum hole concentration of $h^+ \approx 0.7 = 3 \times 0.233$ and a mean cationic charge of $\langle q \rangle_c = 1.738$ could yield a transition temperature near T_{co} = 300 K. The effect of crystal lattice swelling due to large cation substitution may be compensated by a larger permittivity of the compound (see Equation (3)).

Recently I proposed an Cs-elpasolite as candidate for solar cell application, namely $Cs_2(Na,Cu,Ag)_1Bi_1(I,Br)_6$ [14]. What would happen by hole doping of such compound, for instance by substitution of I^{1-} or Br^{1-} by some

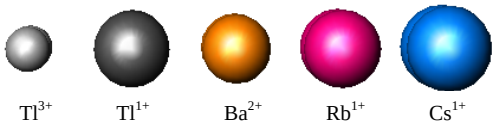

Figure 2. Relative size of cations, if coordinated by six anions. Cation radii in Å: Tl^{3+} 0.89, Tl^{1+} 1.50, Ba^{2+} 1.35, Rb^{1+} 1.52, Cs^{1+} 1.67.

O^{2-}? A chemical content near $Cs_2(Na,Cu,Ag)_1Bi_1(I,Br)_{5.4}(O,S)_{0.6}$ looks very interesting, though it shows an optimum h^+ concentration and would reach a $T_c \approx 370$ K, counting the formally enhanced oxidation state of Cu or Ag, respectively. Alternative sulfide replacement is considered owing to the well adapted ionic radius near that of I^{1-} or Br^{1-}. A vision is that both properties, high solar efficiency and superconductivity, occur together in slightly altered parts of a single compound and can be shared in future.

2.4.2. Nano-Scale Sandwich Structures Based on Tenorite (CuO) Layers

The discovery of multiferroic properties of slightly acentric CuO (tenorite) [40] as well as the formation of elongated rocksalt-type T-CuO thin films onto a (100)-$SrTiO_3$ substrate [41] has increased immensely the interest in these compounds. At low temperature tenorite undergoes two successive magnetic transitions at $T_{N1} = 213$ K and $T_{N2} = 230$ K [40] [42]. Ferroelectric response is indicated at $T_c = 230$ K together with the development of a spiral-magnetic order and spontaneous electric polarization P_s along the *b* axis. Removing of the glide mirror plane would lead to the acentric point group 2. It is natural to identify the temperature of $T_{N2} = 230$ K with the 220 K temperature found for filamentary superconductivity on tenorite samples. However, the intrinsically physical properties and the high permittivity near the phase transition may also support a real superconducting transition, if applied strain would enhance the small concentration of holes that already exists. Notably, the smallest observed Cu-Cu distance of 2.900 Å (**Table A1**) indicates metallic bonding behavior with the ability to create holes.

In tenorite and T-CuO, respectively, are twice as many copper atoms in the atomic layers compared to the CuO_2 nets, and the copper to copper distances are similar to the oxygen-oxygen distances of about 2.73 Å. Both nets are compared in **Figure 3**. T-CuO nets should be investigated in detail to unravel their possible suitability as building units for superconductors. Especially (100) oriented composite structures composed of tenorite (CuO), cuprite (Cu_2O) and metallic AuCu alloy supports will be investigated. In addition, also CuBr or CuI are considered as material using [001] as stack direction.

The monoclinic crystal structure of tenorite is indeed a strongly folded and distorted rocksalt structure formed by unit cell twinning along (010) planes (**Figure 4**).

Twinning of the rocksalt structure type was first described in the system PbS-Bi_2S_3 by the present author and may serve as an example for CuO twinning too, although it does not be "chemical" twinning, because contrary to the PbS-Bi_2S_3 system, the chemical content remains unchanged [43] [44].

Starting with the T-CuO structure, twin-folding to tenorite may be initiated by local Cu^{1+}-Cu^{3+} charge disproportionation, which would remove the *Jahn-Teller* distortion of Cu^{2+} caused by its d^9 electron configuration [45]. Interestingly on this aspect is that the *dd*-excitations of tenorite, characterized by its *UV-VIS* spectrum as well as *EPR* studies, have been interpreted on the basic of a d^2 configuration rather than a d^9 configuration [46]. This suggests dimerization of formally 2+ charged Cu pairs, which may actually considered as Cu^{1+}-Cu^{3+} pairs. Not surprisingly, a very small quantity of Cu^{3+} was found as relict in tenorite [47]. The few attributed holes order themselves in charge stripes along [100] [48]. The hole carriers are obviously sourced out into the (010) twin plane sinks, extending down [100] (see **Figure 4**).

Turning now to copper oxide composites, room temperature superconductivity is proposed for a composition near $6CuO{\cdot}Cu_2O$ with $\langle q \rangle_c \approx 1.75$. A (100)-$SrTiO_3$ substrate may be first coated with an AuCu I thin film, onto which a tenorite layer is deposited along [010], succeeded by a (100)-cuprite layer, and finished by a further tenorite layer in compliance with the stoichiometric specification. The layer sequence may be changed to deposit tenorite between cuprite layers, which can give a distinct result. The [101] direction of tenorite is sought to be oriented parallel to [100] of cuprite. The oxygen atoms on the interface of the tenorite layer will coordinate with copper atoms of the cuprite layer and vice versa (see **Figure 5**).

An open question is, whether self-doping is possible. If cuprite is considered as reservoir layer, one find short

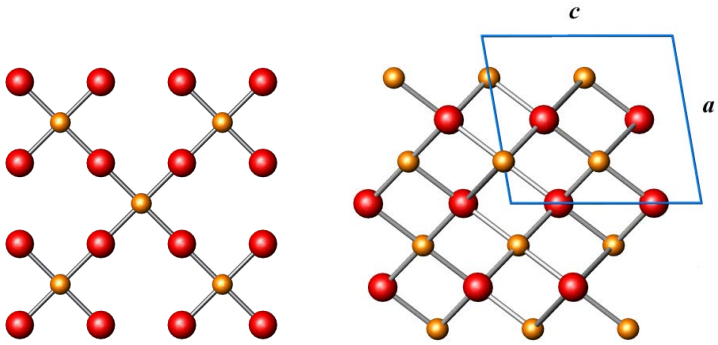

Figure 3. Left: CuO_2 net of high-T_c superconductors. Right: Monoclinic crystal structure of tenorite (CuO), projected down [010] with blue outlined unit cell, copper atoms brownish, oxygen atoms red. The [101] and $[10\bar{1}]$ directions, respectively, corresponding to 45˚ rotation, would yield the rocksalt lattice orientation.

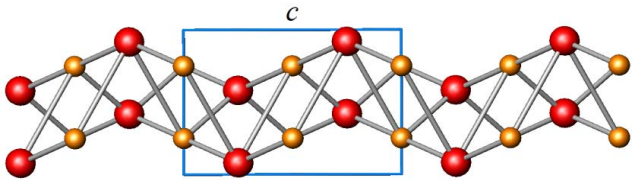

Figure 4. Crystal structure of tenorite, projected onto (100). The drawing clearly indicated that the monoclinic structure is actually a twin-folded and distorted rocksalt structure as already proposed in [10].

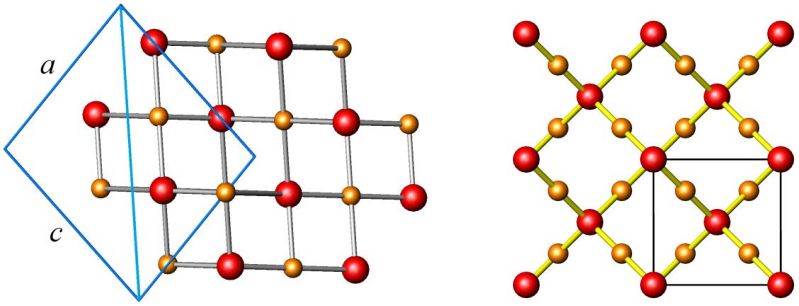

Figure 5. Illustration of the oxygen lattice match between tenorite (left) and cuprite (right), both depicted as projections onto (010). The light blue line in the tenorite picture indicates the [101] direction.

layer distances between copper layers and oxygen layers of $c/4$ = 4.2698/4 Å = 1.0674 Å, whereas the oxygen distances in cuprite are extreme large (**Table 2**). Cu-Cu bonding and d-orbital holes were observed in cuprite, and the four-coordinated oxygen atom is well 2− charged [49]. The copper atoms on the interface of both structures, which are initially 2+ and 1+ charged, respectively, can suffer a formal charge alteration, leading to doping with a sufficient amount of holes. Two processes can deliver holes:

1) Cu-Cu metallic bonding $Cu^{2+} + Cu^{2+} \rightarrow (Cu\text{-}Cu)^{2+} + 2h^{+}$ (formally)

2) Charge disproportionation $6CuO{\cdot}Cu_2O \rightarrow Cu_2O_3{\cdot}2CuO{\cdot}2Cu_2O \rightarrow 4CuO{\cdot}2Cu_2O + 2h^{+}$

The composition is chosen to satisfy the $\langle q \rangle_c = 1.75$ condition for room temperature critical temperature. Strain may well favor charge disproportionation. One can consider the twin planes, depicted in **Figure 6**, as domain walls with soaked holes, showing a wall distance of $d_{(002)}$ = 2.5289 Å. Using these geometrical specifications, hole stripes along [100] and domain extension along [001], respectively, then the [010] direction remains as direction for layer by layer deposition of CuO. If tenorite with its monoclinic angle of β = 99.54˚ is deposited with the *ac* plane onto a tetragonal substrate such as an AuCu alloy, strain can cause multiple twinning along two planes, namely (100) and (001). In this way an incomplete and distorted *Penrose*-like parquet segment can

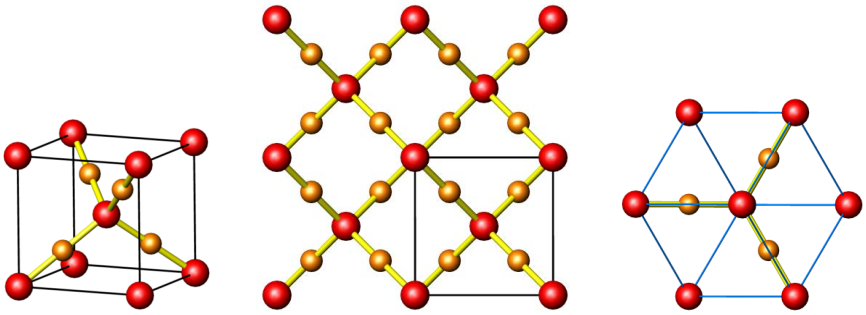

Figure 6. Left: Cubic crystal structure of cuprite (Cu_2O), depicting the characteristic twofold (dumbbell-like) oxygen coordination of Cu^{1+}. Middle: Projection down [100]. Right: Projection down [111].

be formed. In the empty space, corresponding to the acute Penrose tiles, dangling bonds and charge alteration of oxygen, respectively, can easily deliver holes.

Harshman, Fiory and Dow [15] derived another scaling relation to determine the critical temperature of optimum doped superconductors, which exemplarily will be applied to cross check the T_{co} results (**Table 4**).

The *HFD* rule gives

$$T_{co} = 1247.5 \cdot \sqrt{h^+} \big/ \left(d \cdot \zeta\right)(\mathrm{K}), \tag{19}$$

where h^+ is the hole carrier concentration, d (Å) the lattice parameter (Cu-Cu distance in the *ab* plane) and ζ (Å) represents a critical length down the charge reservoir layer, typically the Ba-O distance projected down [001]. This distance roughly corresponds to the *c*-axis coherence length ξ_c. Interestingly, with the change from CuO_2 nets to CuO ones the value of d is reduced by a factor of $\sqrt{2}$, and correspondingly T_{co} would be enhanced by this factor, if the other parameters remain unchanged.

Identifying the lattice plane spacing $d_{(004)}$ = 1.0674 Å of cuprite as the critical length ξ of a "charge reservoir layer", then the *HFD* rule can be applied. **Table 4** summarizes results for specific values chosen, varying the hole concentration and the critical length ξ.

Surprisingly, the mysterious critical temperatures of previous experiments, namely 220 K [3] [4] and about 300 K [5], could be reproduced, thereby explaining their T_{co} ratio of about $\sqrt{2}$. Numerically, room temperature superconductivity seems possible, if these specifications can be realized in practice. Notably, only two copper-oxygen layers are considered to spend optimum holes.

Alternatively, other orientations of thin film deposition may be tested. For instance, (001)-layers of Au or AuCu can be deposited on a cleaved mica sheet, succeeded by a (111)-oriented cuprite layer (see **Figure 4**, right). Then tenorite will be deposited with pseudo-hexagonal layers oriented as in **Figure 7**, followed by another cuprite film.

In this way one avoids that not wanted T-CuO forms at all.

Thus, two possible orientations for epitaxial layer growth of copper oxides are indicated as consequence of this modeling: along (010) of tenorite and along (111) of cuprite, respectively. For an elaborated experiment, also tenorite single crystals could be cut in the wanted orientation. Under less controlled conditions, the deposition of (010)-oriented layers likely happens with unfortunate domain extension normal to the film surface. The extremely short filaments would lead to unstable current transport.

Tetragonal CuO (siemonsite), which may initially be formed, is not wanted because of its large layer separation of c = 5.30 Å. Tetragonal CuO should be given the opportunity to collapse into the "dying swan" structure of tenorite by varying the coating thickness. Also paramelaconite, Cu_4O_{3-x}, is not considered as superconductor material [50]. The data in **Table A1** were reported for purpose of completeness.

Finally, attention needs to be given to nano-structures that may be built up from tenorite and CuI (or CuBr, CuCl), respectively. Adequate doping implied, a composition of 2CuO·CuI with a *Fibonnaci* mean cationic quotient of $\langle q \rangle_c = 5/3$ would be able to reach a transition temperature of $T_c \approx 355$ K. As pursued recently for solar cell application [14], a (111) oriented AuCu alloy support is recommended to deposite (111)-CuI first and then tenorite.

The hypothetical compound $BaCuO_2$ with puckered T-CuO nets [10] may be deposited onto a (100)-AuCu

Table 4. Rough calculation of $T_{co} = 1247.5\sqrt{(nh^+)}/(d \cdot \xi)$ according to the *HFD* rule.

Domain extension d(Å) Tenorite	Critical length ξ (Å) Cuprite	Hole concentration h^+	T_{co} (K)
$d_{(002)}$ = 2.5289	$d_{(004)}$ = 1.0674	0.228	221
		2 × 0.228	312
$d_{(202)}$ = 1.5803	$d_{(222)}$ = 1.2325	0.228	306
		2 × 0.228	433

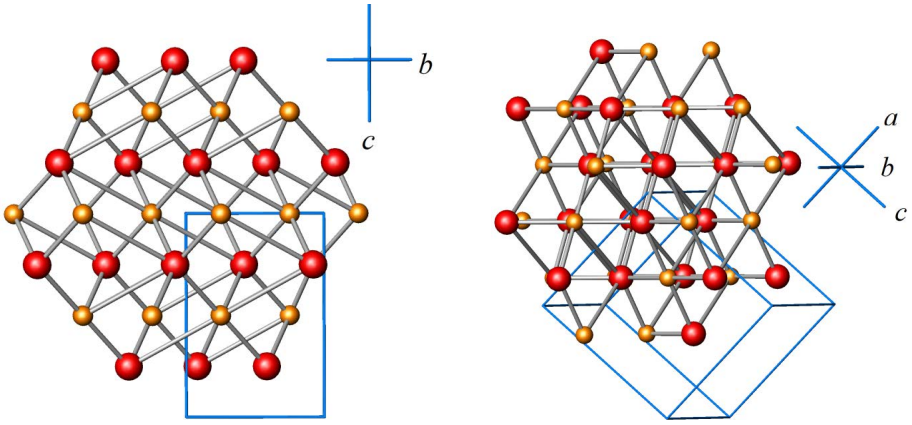

Figure 7. Two selected orientations of tenorite. Left: Atomic layers perpendicular to [001] with layer spacings of $d_{(004)}$ = 1.2645 Å. Right: A tenorite orientation showing pseudo-hexagonal nets as well as atom layers with the lattice plane spacing of $d_{(202)}$ = 1.5803 Å perpendicular to the [101] direction (along the paper long side).

substrate, itself deposited onto (100)-$SrTiO_3$. Cs^{1+} substitution for Ba^{2+} could deliver holes. The mean cationic charge for a composition of $Ba_{0.772}Cs_{0.228}CuO_2$ would yield $\langle q \rangle_c = 1.772$, leading to $T_{co} \approx 278$ K for the assumed critical temperature. However, the critical length ξ down the "charge reservoir" would be too large to uphold this result by an alternative calculation, using the *HFD* rule [15].

In conclusion, there are strong arguments for a reappraisal of tenorite-cuprite as well as tenorite-CuI (CuBr, CuCl) sandwich structures as candidates for room temperature superconductivity.

2.4.3. An Anti-Perovskite Option

Based on the recent investigation of the crystal structure of the H_2S based high-pressure superconductor by Gordon *et al.* [2] the idea ripened to construct a hypothetical anti-perovskite structure, which would fulfill the conditions of low cationic charge. Many years ago, the present author investigated the monoclinic crystal structure of the ferroic compound Pb_3GeO_5 and presented it as anti-perovskite structure type, where the large $(GeO_4)^{4-}$ units occupy the A-sites and $(OPb_3)^{4+}$ the B-site of a perovskite type [51]. According to the investigation of Gordon *et al.* [2] the superconducting H_2S modification may as well be understood as anti-perovskite with $(SH)^-$ occupying the A-site and $(SH_3)^+$ the B-site, respectively.

The Pb_3GeO_5 lead germanate is ferroelastic with a pronounced domain structure. Domains can easily be restored in the other orientation states. When hole doping would be possible, nesting of the charge carriers in the ferroelasic domain wall sinks could be proposed. Crystal-chemically interesting would be a composition of $(SiO_2F_2)^{2-}(BrRb_3)^{2+}$ with a mean cationic charge of $\langle q \rangle_c = 1.75$, leading to a possible transition temperature of $T_{co} \approx 292$ K, if optimal doped. The realization of such compound is doubtful. However, high pressure may be a mean to outsmart limiting factors.

3. Conclusion

From an empirical relation between the critical temperature T_{co} of optimum doped superconductors and the

mean cationic charge $\langle q \rangle_c$ new insights were obtained, which strongly indicate the fractal character of high-T_c superconductivity. The optimum hole concentration of $\sigma_o = 0.229$ can be linked with the universal fractal constant of $\delta_1 = 8.72109$ characteristic for the renormalized quadratic *Hénon* map, giving $\sigma_o = 2/\delta_1$. In addition, the width of superconducting domains is governed by *Fibonacci* numbers, including mixed domain states (applying the mean of consecutive numbers). Inverse scaling with δ_1 also occurs in the gap relation for conventional superconductors, $k_B T_c$ (*BCS*) $\approx 5\Delta_0/\delta_1$. Experiment and theory in this field of science may be steered into new paths, in accordance with fractal conductance behavior and the conjecture that superconductivity may come from the cold. There is evidence to favor low $\langle q \rangle_c$ compounds with high permittivity to reach superconductivity above room temperature. The simple relation $T_{co}(\mathrm{K}) = 2740/\langle q_c \rangle^4$ points to compounds around $\langle q \rangle_c \approx 1.74$ to reach this dream. Some compounds are proposed for experiments. Besides Cs^{1+} substitution in the known Tl-1223 cuprate, especially composites consisting of multiferroic tenorite and cuprite layers, respectively, were recommended because of previously reported filamentary superconductivity of such composites. Tenorite with twice as many copper atoms in the structural layers compared to CuO_2-based nets is highly interesting. Cesium is an element of the green future and has already found its way into smart perovskite solar cells. Modeled on the anti-perovskite high-pressure modification of H_2S, a $(SiO_2F_2)^{2-}(BrRb_3)^{2+}$ anti-perovskite may be a further option for high-T_c. Once again it should be stressed that a low cationic charge is optimal for both solar cells and superconductors.

References

[1] Drozdov, A.P., Eremets, M.I. and Troyan, I.A. (2014) Conventional Superconductivity at 190 K at High Pressure. arXiv:1412.0460 [cond-mat.supr-con], 1-8.

[2] Gordon, E.E., Xu, K., Xiang, H., Bussmann-Holder, A., Kremer, R.K., Simon, A., Köhler, J. and Whangbo, M.H. (2016) Structure and Composition ofthe 200 K-Superconducting Phase of H_2S under Ultrahigh Pressure: The Perovskite $(SH^-)(H_3S^+)$. *Superconductors International Edition*, **128**, 3746-3748.

[3] Schönberger, R., Otto, H.H., Brunner, B. and Renk, K.F. (1991) Evidence for Filamentary Superconductivity up to 220 K in Oriented Multiphase Y-Ba-Cu-O Thin Films. *Physica*, **C173**, 159-162. http://dx.doi.org/10.1016/0921-4534(91)90363-4

[4] Azzoni, C.B., Paravicini, G.B.A, Samoggia, G., Ferloni, P. and Parmigiani, F. (1990) Electrical Instability in CuO_{1-x}: Possible Correlations with the CuO-Based High Temperature Superconductors. *Zeitschriftfür Naturforschung*, **A45**, 790-794. http://dx.doi.org/10.1515/zna-1990-0605

[5] Osipov, V.V., Kochev, I.V. and Naumov, S.V. (2010) Giant Electric Conductivity at the CuO-Cu Interface: HTSL-Like Temperature Variations. *Journal of Experimental and Theoretical Physics*, **93**, 1082-1090. http://dx.doi.org/10.1134/1.1427119

[6] Shevelev, V.V. and Tsoi, T.S. (2010) Electric Current Conductor and Method for the Production Thereof. Patent EP 2169688 A1.

[7] Reyen, N., Thiel, S., Caviglia, A.D., Fitting Kourkoutis, L., Hammerl, G., Richter, C., Schneider, C.W., Kopp, T., Rüetschi, A.S., Jaccard, D., Gabay, M., Muller, D.A., Triscone, J.M. and Mannhart, J. (2007) Superconducting Interface between Insulating Oxides. *Science*, **317**, 1196-1198. http://dx.doi.org/10.1126/science.1146006

[8] Rhim, S.H., Saniz, R., Weinert, M. and Freeman, A.J. (2015) Superconductivity in CuCl/Si: Possible Excitonic Pairing? arXiv:1510.03948v1 [cond-mat.supr-con], 1-5.

[9] Chu, C.W., Rusakov, A.P., Huang, S., Early, S., Geballe, T.H. and Huang, C.Y. (1978) Anomalies in Cuprous Chloride. *Physical Review*, **B18**, 2116. http://dx.doi.org/10.1103/physrevb.18.2116

[10] Otto, H.H. (2015) Modeling of a Cubic Antiferromagnetic Cuprate Super-Cage. *World Journal of Condensed Matter Physics*, **5**, 160-178. http://dx.doi.org/10.4236/wjcmp.2015.53018

[11] Otto, H.H. (2008) Family Tree of Perovskite-Related Superconductors. arXiv:0810.3501v1[cond-mat.supr-con], 1-8.

[12] Kostadinov, I.Z. (2016) 373 K Superconductor. arXiv:1603.01482v1 [phys.ge-ph], 1-10.

[13] Tschauner, O., Ma, C., Beckett, J.R., Prescher, C., Prokapanka, V.B. and Rossman, G.R. (2014) Discovery of Bridgmanite, the Most Abundant Mineral in Earth, in a Shocked Meteorite. *Science*, **346**, 1100-1102. http://dx.doi.org/10.1126/science.1259369

[14] Otto, H.H. (2016) Perovskite Twin Solar Cell with Estimated 50% Bifacial PCE Potential and New Material Options. arXiv:1601.05669 [cond-mat.mtrl-sci], 1-8.

[15] Harshman, D.R., Fiory, A.T. and Dow, J.D. (2011) Theory of High-T_c Superconductivity: Transition Temperature. *Journal of Physics*: *Condensed Matter*, **23**, Article ID: 295701. http://dx.doi.org/10.1088/0953-8984/23/29/295701

[16] Hénon, M. (1976) A Two-Dimensional Mapping with a Strange Attractor. *Communications in Mathematical Physics*, **50**, 69-77. http://dx.doi.org/10.1007/BF01608556

[17] Hellmann, R.H.G. (1980) Self-Generated Chaotic Behavior in Nonlinear Mechanics. In: Cohen, E.G.D., Ed., *Fundamental Problems in Statistical Mechanics*, 5th Edition, North-Holland Publishing Company, Amsterdam, 165.

[18] Savin, D.V., Savin, A.V., Kuznetsov, A.P., Kuznetsov, S.P. and Feudel, U. (2012) The Self-Oscillating System with Compensated Dissipation—The Dymamicsot the Approcimate Discrete Map Dynamical System.

[19] Van der Pol, B. (1922) On Oscillation Hysteresis in a Triode Generator with Two Degrees of Freedom. *The London, Edinburgh and Dublin Philosophical Magazine and Journal of Science*, **43**, 700-719. http://dx.doi.org/10.1080/14786442208633932

[20] Mitin, A.V. (2012) Striped Organization of Hole Excitations and Oxygen Interstitials in Cuprates as a Route to Room-Temperature Superconductivity. *Journal of Superconductivity and Novel Magnetism*, **25**, 1277-1281. http://dx.doi.org/10.1007/s10948-012-1594-1

[21] Fratini, M., Poccia, N., Ricci, A., Campi, G., Burghammer, M., Aeppli, G. and Bianconi, A. (2010) Scale-Tree Structural Organization of Oxygen Interstitials in La_2CuO_{4+y}. *Nature*, **466**, 841-844. http://dx.doi.org/10.1038/nature09260

[22] Poccia, N., Ricci, A. and Bianconi, A. (2011) Fractale Structure Favoring Superconductivity at High Temperature in a Stack of Membranes near a Strain Quantum Critical Point. *Journal of Superconductivity and Novel Magnetism*, **24**, 1195-1200. http://dx.doi.org/10.1007/s10948-010-1109-x

[23] Phillabaum, B., Carlson, E.W. and Dahmen, K.A. (2012) Spatial Complexity Due to Bulk Electronic Nematicity in a Superconducting Underdoped Cuprate. *Nature Communications*, **3**, Article Number: 915. http://dx.doi.org/10.1038/ncomms1920

[24] Phillips, J.C. and Jung, J. (2001) Zigzag Filamentary Theory of Broken Symmetry of Neutron and Infrared Vibronic Spectra of $YBa_2Cu_3O_{6+x}$. arxiv:0103167v1 [cond-mat.supr-con], 1-45.

[25] Phillips, J.C. (2009) Topological Theory of Ceramic High Temperature Superconductors. arxiv:0905.0023v2 [cond-mat.supr-con], 1-14.

[26] Bardeen, J., Cooper, L.N. and Schrieffer, J.R. (1957) Theory of Superconductivity. *Physical Review*, **108**, 1175-1204. http://dx.doi.org/10.1103/PhysRev.108.1175

[27] Muschkolaj, S. (2014) Transition Temperatures. *Journal of Modern Physics*, **5**, 1124-1138. http://dx.doi.org/10.4236/jmp.2014.512115

[28] Wolff, M. (1995) Beyond the Point Particle—A Wave Structure for the Electron. *Galilean Electrodynamics*, **6**, 83-91.

[29] El Naschie, M.S. (2009) The Theory of Cantorian Spacetime and High Energy Particle Physics (An Informal Review). *Chaos, Solitons and Fractals*, **41**, 2635-2646. http://dx.doi.org/10.1016/j.chaos.2008.09.059

[30] Tranquada, J.M., Sternlieb, B.J., Axe, J.D., Nakamura, Y. and Uchida, S. (1995) Evidence for Stripe Correlations of Spin and Holes in Copper Oxide Superconductors. *Nature*, **375**, 561-563. http://dx.doi.org/10.1038/375561a0

[31] Otto, H.H., Zetterer, T. and Renk, K.F. (1988) Crystal Structure of the High-T_c Superconductor $Tl_2Ba_2Ca_2Cu_3O_{10}$. *Naturwissenschaften*, **75**, 509-510. http://dx.doi.org/10.1007/BF00361285

[32] Zetterer, T., Otto, H.H., Lugert, G. and Renk, K.F. (1988) Crystal Chemistry of the $Tl_{2-x}Ba_2Ca_nCu_{n+1}O_{2n+6}$ (n = 0, 1, 2) High-T_c Superconductors. *Zeitschrift für Physik. B, Condensed Matter*, **73**, 321-328. http://dx.doi.org/10.1007/BF01314270

[33] Hertlein, T., Burzlaff, H., Otto, H.H., Zetterer, T. and Renk, K.F. (1989) Structural Refinement of the High-T_c Superconductor $TlBa_2Ca_2Cu_3O_9$. *Naturwissenschaften*, **76**, 170-172. http://dx.doi.org/10.1007/BF00366400

[34] Romberg, H., Nücker, N., Alexander, M., Fink, J., Hahn, D., Zetterer, T., Otto, H.H. and Renk, K.F. (1990) Density and Symmetry of Unoccupied Electronic States of $Tl_2Ba_2CaCu_2O_8$. *Physical Review B*, **41**, 2609-2611. http://dx.doi.org/10.1103/PhysRevB.41.2609

[35] Otto, H.H., Baltrusch, R. and Brandt, H.J. (1993) Further Evidence for Tl^{3+} in Tl-Based Superconductors from Improved Bond Strength Parameters Involving New Structural Data of Cubic Tl_2O_3. *Physica C*, **215**, 205-208. http://dx.doi.org/10.1016/0921-4534(93)90382-Z

[36] Otto, H.H. (2016) Comment and Supplement to Structural Refinement of the High-T_c Superconductor $TlBa_2Ca_2Cu_3O_9$. Researchgate.

[37] Wang, X.G., Hu, P.Y., Huang, Z.M., Wang, R.D. and Gao, X.H. (1994) Effect of F Doping in the (Bi,Pb)-Sr-Ca-Cu-O System. *Physica C*, **233**, 327-331. http://dx.doi.org/10.1016/0921-4534(94)90759-5

[38] Chu, C.W., Gao, L., Chen, F., Huang, Z.J., Meng, R.L. and Xue, Y.Y. (1993) Superconductivity above 150 K in $HgBa_2Ca_2Cu_3O_{8+\delta}$ at High Pressure. *Nature*, **365**, 323-325. http://dx.doi.org/10.1038/365323a0

[39] Monteverde, M., Nunez-Regueiro, M., Acha, C., Lokshin, K.A., Pavlov, D.A., Putilin, S.N. and Antipov, E.V. (2004)

Fluorinated Hg-1223 under Pressure: The Ultimate T_c of the Cuprates? *Physica C*, **408-410**, 23-24. http://dx.doi.org/10.1016/j.physc.2004.02.020

[40] Kimura, T., Sekio, Y., Nakamura, H., Siegrist, T. and Ramirez, A.P. (2008) Cupric Oxide as an Induced-Multiferroic with High-T_c. *Nature Materials*, **7**, 291-294. http://dx.doi.org/10.1038/nmat2125

[41] Siemons, W., Koster, G., Blank, D.H.A., Hammond, R.H., Geballe, T.H. and Beasley, M.R. (2009) Tetragonal CuO: End Member of the 3D Transition Metal Monoxides. *Physical Review B*, **79**, Article ID: 195122. http://dx.doi.org/10.1103/PhysRevB.79.195122

[42] Yang, B.X., Thurston, T.R., Tranquada, J.M. and Shirane, M. (1989) Magnetic Neutron Scattering Study of Single-Crystal Cupric Oxide. *Physical Review B*, **39**, 4343-4349. http://dx.doi.org/10.1103/PhysRevB.39.4343

[43] Otto, H.H. and Strunz, H. (1968) Zur Kristallchemie Synthetischer Blei-Wismutspießglanze. *Neues Jahrbuch für Mineralogie Abhandlungen*, **108**, 1-19.

[44] Otto, H.H. (1984) Neue Erkenntnisse Über Die Verbindungen des Systems PbS-Bi_2S_3 (Und Verwandter Verbindungen). *Zeitschrift der Förderer des Bergbaus und des Hüttenwesens an der Technischen Universität Berlin e.V*, **18**, 1-6. (Researchgate)

[45] Jahn, H.A. and Teller, E. (1937) Stability of Polyatomic Molecules in Degenerate Electronic States. I. Orbital Degeneracy. *Proceedings of the Royal Society A*, **161**, 220-235. http://dx.doi.org/10.1098/rspa.1937.0142

[46] Reddy, R.R.S., Reddy, S.L., Rao, P.S. and Forst, R.L. (2010) Optical Absorption and EPR Studies on Tenorite Mineral. *Spectrochimica Acta Part A*, **75**, 28-31. http://dx.doi.org/10.1016/j.saa.2009.09.009

[47] De Sisto, W., Collins, B.T., Kershaw, R., Dwight, K. and Wold, A. (1989) Preparation and Characterization of Copper(II) Oxide Single Crystals by Chemical Vapor Transport. *Materials Research Bulletin*, **24**, 1005-1010. http://dx.doi.org/10.1016/0025-5408(89)90185-2

[48] Zheng, X.G., Xu, C.N., Tomokiyo, Y., Tanaka, E., Yamada, H. and Soejima, Y. (2000) Observation of Charge Stripes in Cupric Oxide. *Physical Review Letters*, **85**, 5170-5173. http://dx.doi.org/10.1103/PhysRevLett.85.5170

[49] Zuo, J.M., Kim, M., O'Keeffe, M. and Spence, J.C.M. (1999) Direct Observation of *d*-Orbital Holes and Cu-Cu Bonding in Cu_2O. *Nature*, **401**, 49-52. http://dx.doi.org/10.1038/43403

[50] Djurek, D., Prester, M., Drobak, D., Ivanda, M. and Vojta, D. (2014) Magnetic Properties of Nanoscale Paramelaconite Cu_4O_{3-x}. *Journal of Magnetism and Magnetic Materials*, **373**, 183-187.

[51] Otto, H.H. (1979) Die Kristallstruktur der ferroischen Verbindung $Pb_3[O|GeO_4]$. *Zeitschrift für Kristallographie*, **149**, 227-240.

[52] Pearson, W.B. and Vineyard, G.H. (2013) A Handbook of Lattice Spacings of Metals and Structures of Alloys. E-Book Elsevier Reference Monographs.

Appendix

Proper Substrates for Epitaxial Thin Film Growth

A frequently used substrate for epitaxial growth of thin films of superconductors is (100)-$SrTiO_3$. It can be used for the deposition of both types of copper oxide based nets. If one thinks about a metallic substrate, AuCu alloys would be best adapted to an epitaxial growth of any copper oxide composite. Au has the tendency to favor (111) layers, if deposited on smooth surfaces. However, deposition onto a (100)-$SrTiO_3$ would favor (100) growth. The cubic AuCu $L1_0$ phase with an atomic ratio of 1:1 has a lattice parameter of a = 3.859 Å. The atomic distance yields $a/\sqrt{2} = 2.729$ Å. In contrast, the tetragonal AuCu I phase has lattice parameters of a = 3.942 Å and c = 3.670 Å, whereas the AuCu II phase is orthorhombic with lattice parameters of a = 3.946 Å, b = 3.957 Å, and c = 3.646 Å, respectively [52]. The c parameters of the non-cubic phases are similar to the cubic lattice parameter of pure Cu. As a result of these considerations one should choose the AuCu I alloy with its smaller layer separation down [001] of 3.67 Å, because a small layer distance may be important in case such metallic buffer would contribute to superconducting properties. A proper substrate for the deposition of thin films of Cu_2O (cuprite) is (100)-MgO due to its cubic lattice parameter of a = 4.212 Å compared to a = 4.2696 Å for cuprite.

If simply extruded foils of pure copper are used as a substrate for preliminary experiments, their annealing under protective hydrogen atmosphere at 600˚C provides a highly ductile product that does not break, even if most frequently bent.

Table A1. Crystallographic data and physical properties for copper and copper oxides.

Phase	copper	tenorite	"siemonsite"	cuprite	paramelaconite
Formula	Cu	CuO	T-CuO	Cu_2O	Cu_4O_{3-x}
Space group	Fm3m	C2/c (293 K)		Pn3m	$I4_1/amd$
a (Å)	3.6147	4.6837	3.905	4.2696	5.837
b (Å)		3.4226			
c (Å)		5.1288	5.30		9.932
β (°)		99.54			
V (Å^3)		81.080	80.82	77.832	4 × 84.598
ρ (kg/m^3)	8.937	6.516	6.54	6.106	5.93
Cu-Cu (Å)	2.5560	2.9005 3.0830 3.1733	2.761	3.0191	2.9185
ε		5.9 ‖ [010] 6.2 ‖ [101] 7.8 ‖ [10$\bar{1}$]		7.11 $\varepsilon(0)$ 6.46 $\varepsilon(\infty)$	4.24 $\varepsilon(\infty)^*$
Θ_D (K)	347 (0 K) 310 (298 K)	391		188	
v_s (m/s)	4.76 × 10^3 longitudinal 2.33 × 10^3 transverse	6.4 × 10^3 [100] 4.1 × 10^3 [010] 7.8 × 10^3 [001] 5.4 × 10^3 [101] 9.1 × 10^3 [10$\bar{1}$] 6.8 × 10^3 [111]			
T_N (K)		213 230			45 - 55 120
E_g (eV)		1.2		2.137	1.34 (indirect) 2.47 (direct)

*Calculated from the refractivity index. Θ_D *Debye* temperature, v_s sound velocity, ε permittivity, ρ density, T_N *Neel* temperature, E_g energy gap.